

# InterCoG: Towards Spatially Precise Image Editing with Interleaved Chain-of-Grounding Reasoning

Yecong Wan<sup>1</sup> Fan Li<sup>2</sup> Chunwei Wang<sup>2</sup> Hao Wu<sup>1</sup> Mingwen Shao<sup>3</sup> Wangmeng Zuo<sup>1</sup>

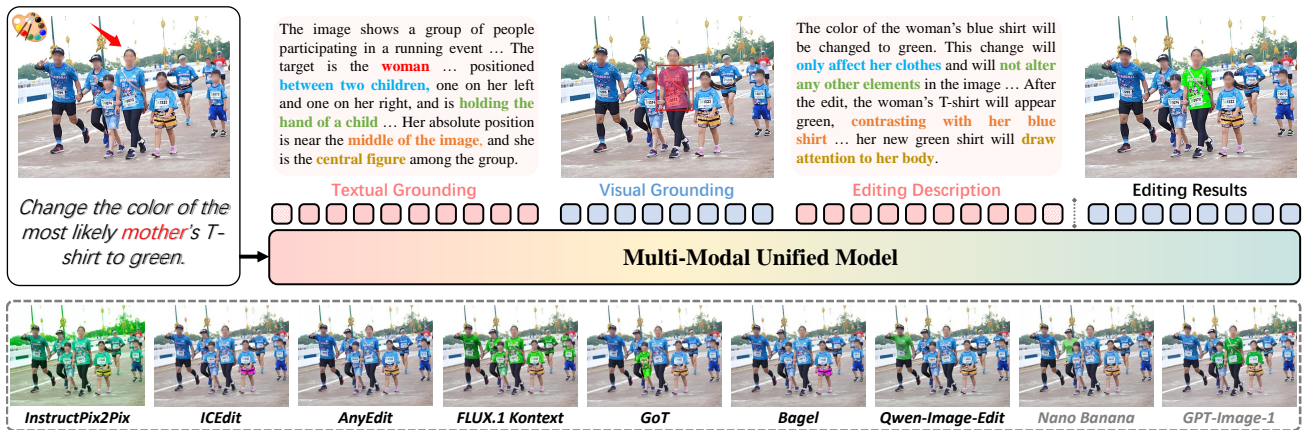


Figure 1. InterCoG, a novel framework that achieves spatially precise image editing in complex scenes via interleaved chain-of-grounding reasoning. InterCoG first conducts position reasoning (textual grounding), highlights the bounding boxes and masks on the image (visual grounding), and then rewrites the editing description to produce the final result. InterCoG achieves superior editing performance compared to state-of-the-art methods. Our results are more precise, making the model highly effective for realistic applications.

## Abstract

Emerging unified editing models have demonstrated strong capabilities in general object editing tasks. However, it remains a significant challenge to perform fine-grained editing in complex multi-entity scenes, particularly those where targets are not visually salient and require spatial reasoning. To this end, we propose InterCoG, a novel text-vision **Interleaved Chain-of-Grounding** reasoning framework for fine-grained image editing in complex real-world scenes. The key insight of InterCoG is to first perform object position reasoning solely within text that includes spatial relation details to explicitly deduce the location and identity of the edited target. It then conducts visual grounding via highlighting the editing targets with generated bounding boxes and masks in pixel space, and finally rewrites the editing description to specify the intended outcomes. To further facilitate this paradigm, we propose two auxiliary training modules: multimodal grounding recon-

struction supervision and multimodal grounding reasoning alignment to enforce spatial localization accuracy and reasoning interpretability, respectively. We also construct GroundEdit-45K, a dataset comprising 45K grounding-oriented editing samples with detailed reasoning annotations, and GroundEdit-Bench for grounding-aware editing evaluation. Extensive experiments substantiate the superiority of our approach in highly precise edits under spatially intricate and multi-entity scenes.

## 1. Introduction

Instruction-based image editing methods have emerged as a powerful tool to provide users with a flexible way to modify images (e.g., object addition, removal, color change, etc.) through textual prompts (Brooks et al., 2023; Zhang et al., 2023a; Yu et al., 2025; Ge et al., 2024). Despite this, existing methods still face challenges: how to enable the model to not only reason about latent editing intentions but also found the precise localization of the target editing region.

Most diffusion-based works (Li et al., 2024; Brooks et al., 2023; Zhang et al., 2023a; Batifol et al., 2025), leveraging text encoders such as CLIP (Radford et al., 2021) or T5 (Raffel et al., 2020). Nevertheless, these models struggle

<sup>1</sup>Harbin Institute of Technology <sup>2</sup>Huawei Noah's Ark Lab  
<sup>3</sup>Shenzhen University of Advanced Technology. Correspondence to: Wangmeng Zuo <wmzuo@hit.edu.cn>.

to infer complex user intentions and lack sufficient multi-modal grounding capabilities, which constrains their ability to achieve faithful, fine-grained editing.

More recently, unified multi-modal generation frameworks (Wu et al., 2025a; Liu et al., 2025; Lin et al., 2025; Chen et al., 2025b; Deng et al., 2025; Pan et al., 2025; Wang et al., 2025; OpenAI, 2025a) have adopted large multimodal language models (MLLMs) as text encoders and exhibit unprecedented capabilities in complex instruction-based editing with high fidelity and quality. Despite these advances, current methods primarily excel at editing relatively salient or explicitly described targets. In addition, recent efforts have explored region-aware editing via pre-extracted candidate regions (Zhou et al., 2025), explicit coordinate prediction (Fang et al., 2025; Qu et al., 2025), or coarse mask-based localization (Zou et al., 2025). However, these explicit geometric cues often prove coarse and unreliable, failing to satisfy the demands of multi-subject scenes that require implicit, reasoning-based grounding cues for the target editing regions.

To address the aforementioned challenges, we propose **InterCoG**, a novel text–vision **Interleaved Chain-of-Grounding** framework that enables precise editing for subjects and regions based on the context of implicit reasoning. Specifically, InterCoG first performs object position reasoning solely within the text modality; that is, it deduces spatial relation details to clarify the location and identity of the edited targets. Following this, InterCoG performs visual grounding by highlighting the targets with generated bounding boxes and masks in the pixel space, and finally rewrites the editing description to specify the intended outcomes. By interleaving these three fine-grained textual and visual localization cues, our method establishes a specific reasoning trajectory that accurately anchors editable areas, ensuring that edits remain semantically faithful and spatially consistent. To further facilitate this paradigm, we introduce two auxiliary training modules: multimodal grounding reconstruction supervision and multimodal grounding reasoning alignment. The former enables the model to enhance its object grounding capabilities via mask decoding, while the latter explicitly aligns the features of the target regions with text–vision grounding cues. This thereby enhances the interpretability and spatial alignment of the reasoning process.

To facilitate grounding-oriented and fine-grained editing, we construct GroundEdit-45K, which contains 45K editing samples. Each sample is annotated with detailed text–vision chain-of-grounding annotations, where every editing target is provided with precise bounding-box and mask tags. Furthermore, we introduce GroundEdit-Bench to evaluate models’ capabilities in complex, grounding-aware editing. Comprehensive experiments substantiate the superiority of InterCoG over alternatives under a variety of real-world

challenging conditions.

In conclusion, the main contributions are as follows.

- We propose InterCoG, an innovative interleaved chain-of-grounding reasoning framework that enables fine-grained editing in semantically dense and compositionally complex scenes.
- We introduce two auxiliary training modules - multimodal grounding reconstruction supervision and multimodal grounding reasoning alignment - to enhance spatial localization accuracy and reasoning interpretability.
- We construct GroundEdit-45K, comprising 45K samples with explicit chain-of-grounding annotations, and GroundEdit-Bench for benchmarking grounding-aware editing.
- Our InterCoG demonstrates significant improvements in challenging grounding-oriented editing, substantially outperforming existing methods across various real-world complex scenarios.

## 2. Related Work

### 2.1. Instruction-based Image Editing

Instruction-based image editing demands models to interpret nuanced user intentions and execute edits with high semantic fidelity and spatial precision. Pioneering works such as InstructPix2Pix (Brooks et al., 2023), MagicBrush (Zhang et al., 2023a), and BrushEdit (Li et al., 2024) learn paired instruction–edit mappings with diffusion models but lack explicit instruction representation learning, resulting in shallow semantic understanding and limited alignment with fine-grained user intent. Subsequent efforts including AnyEdit (Yu et al., 2025), UltraEdit (Zhao et al., 2024), EmuEdit (Sheynin et al., 2024), and ICEdit (Zhang et al., 2025) extend this paradigm through larger datasets and refined architectures, yet they remain limited to handling complex instructions and intricate image compositions. The recent emergence of GPT-4o (OpenAI, 2025a) underscores the advantages of unifying visual understanding and generation. Parallel efforts either harness the instruction comprehension capacity of MLLMs as control interfaces for generative models (Lin et al., 2025; Wu et al., 2025b;a; Chen et al., 2025b; Ge et al., 2024) or pursue intrinsically unified multimodal architectures (Deng et al., 2025; Xie et al., 2024; Ma et al., 2025), collectively advancing the fidelity and controllability of instruction-driven editing and ushering in semantically coherent visual generation. Despite this progress, current models typically excel at identifying “what to edit” but often fail to reason “where to edit”, leading to suboptimal target grounding and degraded editing quality in complex multi-subjects scenes.

## 2.2. Textual and Visual Chain of Thought

Large Language Models (LLMs) have exhibited exceptional reasoning abilities through chain-of-thought (CoT) reasoning (Wei et al., 2022), enabling the decomposition of complex tasks into transparent intermediate steps. A surge of recent studies (Mitra et al., 2024; Zhang et al., 2023b; Zheng et al., 2023; Gupta & Kembhavi, 2023; Surís et al., 2023; Hu et al., 2024; OpenAI, 2025b) extend CoT reasoning into the multimodal domain by introducing explicit visual operations, enabling coherent vision–language reasoning with interpretable spatial manipulation, such as cropped, rotated, or zoomed views. Beyond question answering, GoT (Fang et al., 2025) exploits MLLMs to jointly reason about spatial semantics and scene layout, while ReasonBrain (He et al., 2025) repurposes MLLMs for reasoning-driven editing via reasoning cue extraction and cross-modal enhancement. Draw-In-Mind (Zeng et al., 2026) and EditThinker (Li et al., 2025b) further re-plans editing operations by reformulating the instruction through imagination-based reasoning. With the rapid evolution of unified multimodal models, interleaved text–vision reasoning has emerged (Li et al., 2025a; Shi et al., 2025; Qin et al., 2025; Zou et al., 2025; Huang et al., 2026). For instance, UniCoT (Qin et al., 2025) performs iterative self-reflection to refine generation quality. MURE (Zou et al., 2025) integrates interleaved multimodal generation for image editing, yet still struggles with referential reasoning and pixel-level grounding in compositional complex scenes. Moreover, most existing frameworks lack explicit mechanisms to align intermediate reasoning with final outcomes, leading to reasoning–output inconsistencies that underexploit the full potential of CoT reasoning.

## 3. Methodology

Editing real-world images often entails scenes that comprise multiple entities, overlapping elements, and complex spatial arrangements. However, despite the remarkable visual quality achieved by recent image editing methods (Lin et al., 2025; Wu et al., 2025b;a), they typically struggle to accurately localize the referential targets under such challenging conditions. To address these challenges, we introduce InterCoG, a text–vision interleaved chain-of-grounding paradigm that alternately exploits the logical reasoning ability of text and the fine-grained spatial grounding capability of vision, enabling spatially precise and interpretable editing in complex real-world scenarios.

As illustrated in Fig. 1, the interleaved chain-of-grounding paradigm unfolds through four major steps: **(1)** The model first analyzes the input image and instruction to infer the user-intended editing target, producing a textual-level scene understanding and position description; **(2)** Guided by this reasoning, it performs visual grounding by generating an image annotated with a red bounding box and a semi-

transparent mask, precisely perceiving and localizing the desired targets; **(3)** The model subsequently constructs a fine-grained editing description accompanied by an outcome rationale; and **(4)** the interleaved reasoning chain ultimately directs the model to execute final editing.

By interleaving linguistic reasoning and spatial grounding, InterCoG establishes a coherent bridge between referential comprehension and localized visual manipulation, achieving fine-grained, semantically faithful edits across complex multi-entity scenarios. We next introduce the key elements of our paradigm: dataset construction and framework.

### 3.1. Grounded Editing Dataset Construction

Existing image editing datasets primarily focus on salient objects or prominent regions, offering limited coverage of fine-grained and contextually entangled targets. To bridge this gap and support our proposed chain-of-grounding paradigm, we construct GroundEdit-45K, a meticulously crafted dataset comprising 45K grounded editing samples, each equipped with natural language instructions, text–vision interleaved chain-of-grounding annotations, and corresponding images.

As illustrated in Fig. 2, we adopt SAM-1B (Kirillov et al., 2023) as the source of raw images, given its rich diversity in spatial layouts, multi-entity compositions, and large-scale real-world scenes. In contrast to prior datasets such as ImgEdit (Ye et al., 2025), which first define editing targets and then perform grounding, our setting focuses on complex multi-entity scenarios in which existing grounding models (Lai et al., 2024; Ren et al., 2024) often fail to accurately localize the desired targets. To ensure precise grounding annotations, we adopt a grounding-first strategy: the entire scene is first grounded, after which specific editing targets are selected from the grounded entities to prompt MLLMs to generate the corresponding editing instructions.

**Step 1.** We begin by identifying all potential objects using the Recognize Anything Model (RAM) (Huang et al., 2025), followed by Grounded-SAM (Ren et al., 2024) to localize all detected entities across the image, yielding corresponding bounding boxes and segmentation masks. We filter out low-confidence predictions and randomly select one remaining object as the editing target. To ensure that the selected targets exhibit non-trivial grounding difficulty rather than trivial recognition, we employ Qwen2.5-VL-7B (Bai et al., 2025) to filter out overly salient instances. The final visual grounding is then defined as the grounded image itself, with the target highlighted by a red semi-transparent mask (opacity 0.5) and a red bounding box.

**Step 2.** We overlay the bounding box of the selected target onto the original image and prompt Qwen2.5-VL-72B (Bai et al., 2025) with predefined editing types to generate the

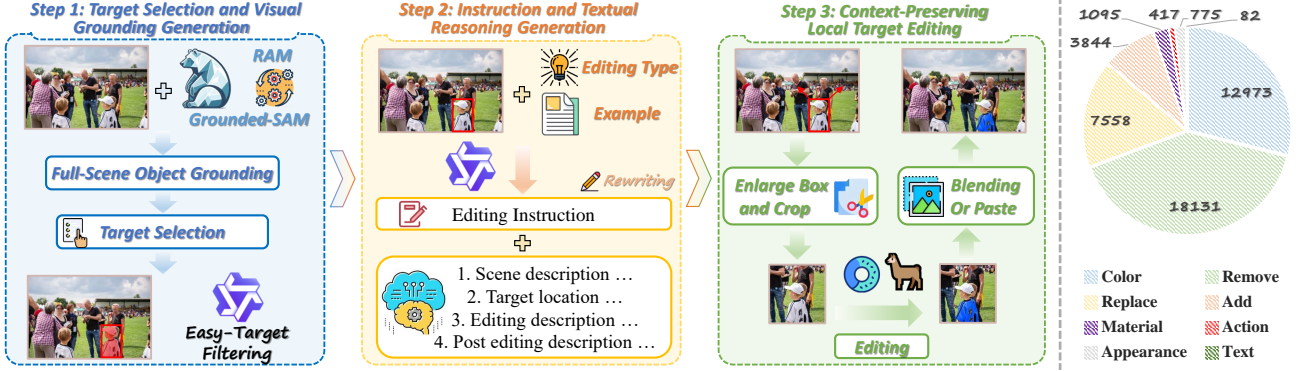


Figure 2. **GroundEdit-45K Dataset Construction Pipeline and Statistics.** **Left:** The pipeline consists of three steps: (1) target selection and visual grounding generation; (2) instruction and text reasoning generation; and (3) context-preserving local target editing. **Right:** Our dataset contains 45K samples covering 8 categories of local editing types.

editing instruction together with its structured textual reasoning. Each reasoning instance consists of four components: (1) scene description, (2) target localization, (3) editing description, and (4) post editing description. Among them, (1) and (2) constitute the first reasoning stage, focusing on referential and spatial comprehension, while (3) and (4) form the second reasoning stage, describing the editing intent and the expected visual outcome. To encourage reasoning-aware instruction generation, we prompt the model to produce instructions such as “Turn the clothes of the person facing to the left to blue.”, where identifying the correct target requires resolving multi-entity spatial relations rather than trivial object naming. Qwen3 (Yang et al., 2025) is further employed to rewrite and paraphrase the generated instructions, yielding more natural and varied expressions.

**Step 3.** To guarantee that the designated target is accurately modified, we first crop the region specified by its bounding box and apply Bagel (Deng et al., 2025) for localized editing. The edited patch is then reintegrated into the original image via blending, ensuring natural boundary transitions and overall visual consistency. For removal tasks, we employ the target mask with LaMa (Suvorov et al., 2022) to synthesize content-consistent inpainting results, whereas for other editing types, Bagel is used to generate the corresponding modifications. Finally, all edited samples undergo quality filtering via Qwen2.5-VL-7B (Bai et al., 2025), resulting in a curated set of 45K high-quality grounded editing samples.

### 3.2. Interleaved Chain-of-Grounding Framework

Our framework utilizes a state-of-the-art unified model Bagel (Deng et al., 2025) as the backbone, chosen for its outstanding multimodal generation capabilities.

*Preliminaries:* Bagel comprises an understanding expert, built from understanding blocks, and a generation expert, constructed from generation blocks. The two experts share self-attention to enable cross-modal interaction and are responsible for text and vision generation, respectively. Dur-

ing inference, text is produced autoregressively following the next-token prediction paradigm, while images are synthesized by predicting velocity vectors within the rectified flow framework.

The schematic illustration of the proposed InterCoG is depicted in Fig. 3. Given an input image and an editing instruction, InterCoG iteratively produces a text–vision interleaved reasoning sequence within `<think></think>` tokens. Specifically, the unified model first performs **textual grounding reasoning**, interpreting the user’s editing intent and conducting spatial reasoning to derive an explicit description of the target’s location. It then carries out **visual grounding reasoning** to precisely delineate the target regions via pixel-level position annotations. Subsequently, guided by detailed editing descriptions and outcome interpretations, the model generates the final edited image, thus completing the reasoning–grounding–generation chain and enabling fine-grained and semantically aligned editing.

**Multimodal Grounding Reconstruction Supervision.** To further enhance localization capabilities during reasoning and editing, we introduce an auxiliary grounding supervision with a mask reconstruction objective. This supervision employs a shared mask decoder to reconstruct the binary mask conditioned on both textual and visual representations, compelling the model to capture more intrinsic grounding features and achieve more precise edits. Moreover, by sharing the decoder across modalities, the framework naturally aligns textual and visual representations, allowing the model to leverage textual reasoning to improve visual grounding and editing fidelity.

Concretely, we utilize the last hidden states from three sources: (1) text tokens  $H_t$  for textual grounding reasoning, (2) noised VAE tokens  $H_v$  for visual grounding reasoning, and (3) noised VAE tokens  $H_e$  for editing results generation. Each hidden state is processed by a three-layer modality-specific projector,  $TP(\cdot)$  for text and  $VP(\cdot)$  for vision, producing the conditioning features  $C_t$ ,  $C_v$ , and  $C_e$ .

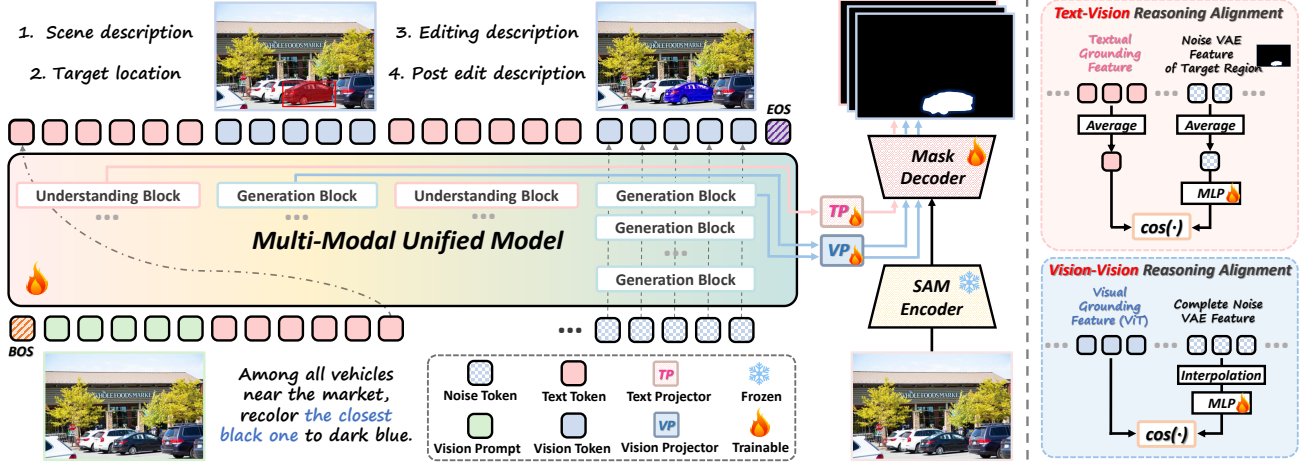


Figure 3. **Overview of the Proposed InterCoG Framework.** **Left:** Our framework performs text–vision interleaved chain-of-grounding reasoning to interpret and locate user-intended targets and formulate editing descriptions, ultimately producing precise and semantically aligned editing results. **Right:** Illustration of the proposed text–vision and vision–vision reasoning alignment schemes, designed to enforce coherent multimodal grounding reasoning.

These features serve as conditions for a shared mask decoder, which predicts the target masks  $\hat{M}_t$ ,  $\hat{M}_v$ , and  $\hat{M}_e$  from the SAM-encoded image features  $E$ . Specifically, the text-based feature  $C_t$  is averaged to yield a single embedding and incorporated through cross-attention, whereas the spatial features  $C_v$  and  $C_e$  are directly added to  $E$ , enabling spatially-aware conditioning:

$$\begin{aligned} \hat{M}_t &= \text{MaskDecoder}(E, C_t), C_t = TP(H_t), \\ \hat{M}_v &= \text{MaskDecoder}(E, C_v), C_v = VP(H_v), \\ \hat{M}_e &= \text{MaskDecoder}(E, C_e), C_e = VP(H_e). \end{aligned} \quad (1)$$

The predicted masks are supervised by the ground-truth binary mask  $M$  using binary cross-entropy (BCE) loss:

$$\mathcal{L}_{mask} = \text{BCE}(\hat{M}_t, M) + \text{BCE}(\hat{M}_v, M) + \text{BCE}(\hat{M}_e, M). \quad (2)$$

**Multimodal Grounding Reasoning Alignment.** Although the chain-of-grounding paradigm offers an interpretable view into the model’s intermediate grounding process, it may suffer from shortcut reasoning, resulting in discrepancies between the inferred location and the actual editing behavior. To explicitly enforce the model to perform reasoning-consistent editing guided by multimodal grounding cues, we propose a grounding reasoning alignment scheme that regularizes the consistency between the editing features and the multimodal grounding representations. This alignment constrains the model to execute its editing based on the regions inferred during reasoning, thereby ensuring spatially faithful and reasoning-consistent modifications.

More concretely, as illustrated on the right side of Fig. 3, we perform two types of alignment: text–vision reasoning alignment and vision–vision reasoning alignment. Our alignment is conducted at a specific transformer layer; hence, we omit the layer index  $l$  for notational simplicity. For the text–vision reasoning alignment, we first compute the av-

erage of the token features corresponding to “2. Target location” in the textual grounding reasoning, denoted as  $G_t^{avg}$ . In parallel, we extract the noised VAE tokens from the editing region specified by the mask and compute their average to obtain  $N_r^{avg}$ . The noised representation  $N_r^{avg}$  is then projected via a learnable MLP,  $P_t(\cdot)$ , and the resulting embedding is then aligned with the text-derived grounding cues  $G_t^{avg}$  by maximizing the cosine similarity:

$$\begin{aligned} G_t^{avg} &= \text{Average}(G_t), \quad N_r^{avg} = \text{Average}(N_r), \\ \mathcal{L}_{tv} &= -\cos(P_t(N_r^{avg}), G_t^{avg}), \end{aligned} \quad (3)$$

where  $\cos(\cdot, \cdot)$  denotes cosine similarity.

Similarly, for vision–vision reasoning alignment, we leverage the ViT token representations (Deng et al., 2025) of the grounded images produced by visual grounding reasoning, denoted as  $G_v^{vit}$ . These tokens encode richer contextual and spatial semantics than their VAE counterparts, providing a more expressive basis for aligning visual features. To establish spatial correspondence, the noised VAE editing features  $N$  are first interpolated to the spatial resolution of  $G_v^{vit}$  and subsequently projected through a learnable MLP,  $P_v(\cdot)$ . We then apply a cosine similarity loss to align the two representations, thereby enforcing spatially grounded coherence between the visual grounding reasoning and the editing features:

$$\begin{aligned} N^r &= \text{Interp}(N, \text{size}(G_v^{vit})), \\ \mathcal{L}_{vv} &= -\frac{1}{I} \sum_{i=1}^I \cos(P_v(N^r), G_v^{vit}), \end{aligned} \quad (4)$$

where  $i$  is the patch index. We apply the reasoning alignment loss at an intermediate transformer layer (i.e., 14), which not only provides meaningful location guidance for the subsequent layers but also allows them to focus more effectively on appearance refinement and content generation.

Table 1. Quantitative comparison on the proposed GroundEdit-Bench. EGA and ES denote the editing grounding accuracy and editing score, respectively. The ‘‘Average’’ column indicates the overall mean across all samples, rather than the mean of the listed categories.

Method	Color Change		Remove		Replace		Add		Appearance		Others		Average		
	EGA↑	ES↑	EGA↑	ES↑	EGA↑	ES↑	EGA↑	ES↑	EGA↑	ES↑	EGA↑	ES↑	EGA↑	ES↑	Human↑
FLUX.2 [Pro]	0.51	2.54	0.59	2.53	0.44	2.70	0.63	3.00	0.22	3.33	0.33	3.00	0.52	2.61	7.3
GPT-Image-1	0.64	2.72	0.71	2.84	0.51	3.25	0.39	2.75	0.80	3.67	0.62	3.67	0.64	2.87	8.2
GPT-Image-1.5	0.80	4.14	0.86	3.77	0.85	3.80	0.84	3.50	0.92	3.67	0.86	4.00	0.83	3.95	8.9
Nano Banana	0.59	2.86	0.63	3.10	0.50	2.60	0.42	2.50	0.74	4.00	0.62	3.33	0.59	2.94	7.9
Nano Banana Pro	0.86	4.16	0.82	3.90	0.82	4.00	0.86	3.75	0.95	3.33	0.93	4.33	0.85	4.03	9.3
InstructPix2Pix	0.11	1.20	0.09	1.13	0.05	1.00	0.14	1.75	0.12	1.00	0.03	1.00	0.10	1.17	2.1
MagicBrush	0.21	1.20	0.13	1.43	0.15	1.40	0.10	1.75	0.11	1.00	0.29	2.33	0.17	1.34	1.9
AnyEdit	0.21	1.30	0.12	1.33	0.15	1.30	0.08	1.00	0.10	2.00	0.07	2.00	0.17	1.40	2.5
ICEdit	0.26	1.40	0.31	1.33	0.26	1.60	0.21	1.75	0.55	1.67	0.31	3.00	0.28	1.47	3.0
GoT	0.48	2.48	0.53	2.37	0.46	3.30	0.29	2.75	0.81	3.33	0.57	2.33	0.50	2.57	5.6
UniWorld-v1	0.31	1.72	0.42	1.77	0.37	2.60	0.57	2.75	0.15	2.00	0.19	2.00	0.35	1.85	4.3
Step1X-Edit	0.53	2.12	0.52	2.17	0.48	2.50	0.59	3.25	0.69	3.33	0.47	3.00	0.53	1.95	4.8
OmniGen2	0.24	1.88	0.35	1.53	0.24	2.25	0.09	1.75	0.09	3.33	0.09	2.33	0.27	1.87	4.5
FLUX.1 Kontext [Dev]	0.39	1.40	0.48	1.98	0.35	2.50	0.60	3.00	0.05	3.33	0.17	3.67	0.40	1.87	5.0
Qwen-Image-Edit	0.52	2.56	0.68	3.27	0.57	3.40	0.40	2.50	0.52	4.00	0.60	3.33	0.57	2.92	8.1
Bagel	0.65	2.68	0.62	2.67	0.52	2.40	0.25	2.50	0.77	2.33	0.64	3.00	0.62	2.65	6.7
Bagel-think	0.56	2.40	0.58	2.50	0.40	2.30	0.25	1.75	0.67	3.00	0.43	3.00	0.54	2.43	6.3
Bagel-SFT	0.73	2.94	0.74	3.23	0.63	3.60	0.66	3.00	0.81	4.00	0.77	3.67	0.70	3.15	8.5
<b>InterCoG (Ours)</b>	<b>0.84</b>	<b>4.08</b>	<b>0.88</b>	<b>3.84</b>	<b>0.89</b>	<b>3.90</b>	<b>0.90</b>	<b>3.75</b>	<b>0.99</b>	<b>4.00</b>	<b>0.92</b>	<b>4.00</b>	<b>0.88</b>	<b>3.97</b>	<b>9.2</b>

**Training and Inference.** During training, the model is optimized with a cross-entropy loss  $\mathcal{L}_{ce}$  for text token prediction. For visual generation, we adopt the Rectified Flow paradigm, supervising the network to predict the velocity field along a straight-line trajectory using a mean squared error loss  $\mathcal{L}_{mse}$ . In addition, the aforementioned losses  $\mathcal{L}_{tv}$ ,  $\mathcal{L}_{vv}$ , and  $\mathcal{L}_{mask}$  are incorporated, yielding the overall training objective:

$$\mathcal{L} = \mathcal{L}_{ce} + \mathcal{L}_{mse} + \lambda_{tv}\mathcal{L}_{tv} + \lambda_{vv}\mathcal{L}_{vv} + \lambda_{mask}\mathcal{L}_{mask}, \quad (5)$$

where  $\lambda_{tv}$ ,  $\lambda_{vv}$ , and  $\lambda_{mask}$  are scaling factors, set empirically to 1.0, 1.0, and 0.1. During inference, the model relies solely on the main network to autoregressively generate an interleaved sequence of text and images, discarding all auxiliary modules and projection layers.

## 4. Experiments

### 4.1. Implementation Details

We initialize our framework with pretrained Bagel weights and train it on the GroundEdit-45K dataset, augmented with additional general understanding, generation, and editing data (Byeon et al., 2022; Gu et al., 2022; Chen et al., 2025a; Schuhmann et al., 2022; Sharma et al., 2018; Sun et al., 2023; Schuhmann et al., 2022) to preserve the base model’s capabilities. The system prompt governs whether the model operates in grounding reasoning mode. Training is conducted for 4K iterations with a batch size of 64 and a learning rate of  $2 \times 10^{-5}$ . To benchmark grounding-aware editing, we introduce GroundEdit-Bench, comprising 100 real-world cases with meticulously human-annotated

instructions and target bounding boxes, ensuring rigorous evaluation of localization and editing accuracy.

### 4.2. Comparisons with State-of-the-Arts

**Comparisons on the Proposed GroundEdit-Bench.** To rigorously evaluate the effectiveness of InterCoG, we conduct a comprehensive comparison against state-of-the-art instruction-based editing methods, as summarized in Tab. 4. We report two metrics: *Editing Grounding Accuracy (EGA)*, which measures the proportion of the edited region (absolute difference before and after editing) that falls within the target bounding box, and *Editing Score (ES)*, which evaluates overall editing quality on a 1–5 scale via GPT-4o, jointly considering visual fidelity and grounding precision. We also report mean human ratings on a 1–10 scale. As can be found, InterCoG achieves unprecedented performance, outperforming all competitors. Notably, it surpasses the top-performing baseline Bagel (Deng et al., 2025) by 0.25 in grounding accuracy and exceeds Qwen-Image-Edit by 1.05 in overall editing quality, demonstrating its superior ability to leverage interleaved reasoning for precise interpretation of user intention and pinpoint execution of edits. Although GoT (Fang et al., 2025) employs textual reasoning for target localization, its reliance on MLLM-based coordinate estimation yields coarse and inaccurate grounding, while the decoupled design between grounding and generation further leads to suboptimal editing results.

We also demonstrate visual comparisons in Fig. 4 and Fig. 5. As suggested, our method precisely interprets user-referred targets and performs interleaved grounding reasoning to

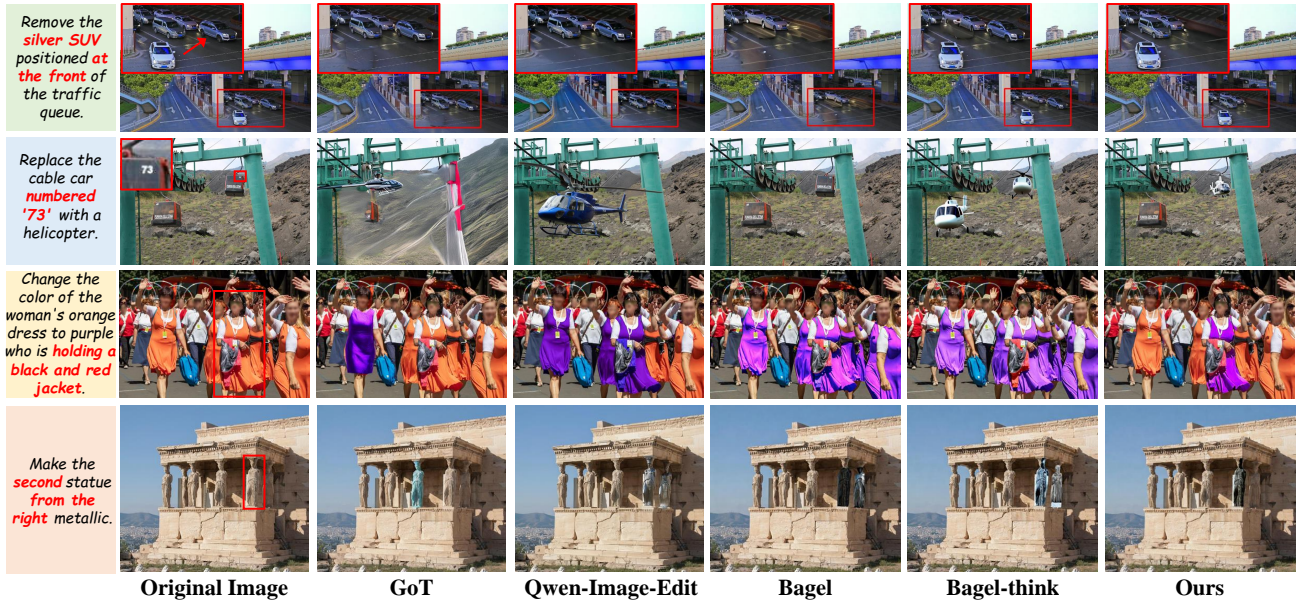


Figure 4. Qualitative comparisons on our proposed GroundEdit-Bench. Our method consistently delivers highly precise and spatially accurate edits, particularly in multi-entity and fine-grained reasoning scenarios. **Best viewed at screen!**

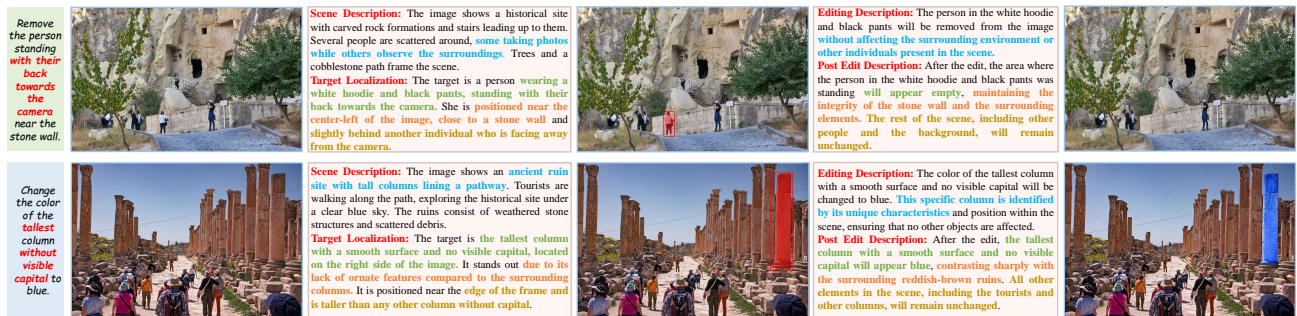


Figure 5. Visualization of the interleaved localization chain-of-thought reasoning processing. InterCoG first interprets user-intended referential targets via textual reasoning and then highlights the object via visualizing bounding boxes and masks in pixel space. By interleaving these multimodal grounding cues, InterCoG is able to precisely locate the editing regions and achieve spatially exact modifications. The editing results of competing methods can be found in the appendix. **Best viewed at screen!**

achieve precise editing on the desired target. In contrast, existing approaches often fail to resolve referential intent, leading to unintended modifications across multiple entities.

**Comparisons on Existing Dataset.** Furthermore, we evaluate InterCoG on the reasoning scenarios of the SmartEdit benchmark (Huang et al., 2024) to more comprehensively validate its effectiveness. As summarized in Tab. 2, InterCoG delivers clear and consistent gains in PSNR, SSIM, LPIPS, and CLIP Score. These improvements confirm that our textual reasoning mechanism correctly infers user-intended targets, while the pixel-level grounding mechanism ensures highly accurate localization of the editable targets. This interleaved design enables precise editing in complex reasoning scenarios while preserving the surrounding context with minimal disturbance. In contrast, existing methods often suffer from reasoning failures that lead to incorrect target localization, and MURE’s coarse-grained localization paradigm also results in suboptimal grounding precision.

More experimental results on SmartEdit’s understanding scenarios and on GEdit-Bench (Liu et al., 2025) are provided in the appendix.

Table 2. Quantitative comparison results on SmartEdit benchmark.

Method	SmartEdit Reasoning Scenarios			
	PSNR $\uparrow$	SSIM $\uparrow$	LPIPS $\downarrow$	CLIP Score $\uparrow$
InstructPix2Pix	24.234	0.707	0.083	19.413
MagicBrush	22.101	0.694	0.113	19.755
InstructDiffusion	21.453	0.666	0.117	19.523
SmartEdit-7B	25.258	0.742	0.055	20.950
SmartEdit-13B	25.757	0.747	0.051	20.777
Bagel	28.076	0.839	0.060	20.767
MURE	28.694	0.883	0.062	21.298
<b>InterCoG (Ours)</b>	<b>30.024</b>	<b>0.901</b>	<b>0.045</b>	<b>21.314</b>

### 4.3. Ablation Studies

In Tab. 3, we conduct ablation experiments on the components introduced in InterCoG. The effectiveness of each

component in InterCoG is evaluated by excluding it from the model, revealing their individual contributions to the overall performance. More detailed analyses are as below.

Table 3. Ablation studies on our proposed GroundEdit-Bench.

Variant	EGA $\uparrow$	ES $\uparrow$
w/o Reasoning	0.70	3.15
w Text-Only Grounding Reasoning	0.76	3.57
w Vision-Only Grounding Reasoning	0.74	3.23
w/o Grounding Reconstruction	0.85	3.83
w/o Reasoning Alignment	0.83	3.71
InterCoG (Ours)	0.88	3.97

### Effect of Interleaved Chain-of-Grounding Reasoning.

As shown in Tab. 3 and Fig. 6, relying solely on textual grounding reasoning allows the model to parse user-referred targets but suffers from coarse positional granularity, often failing to accurately localize the intended editing regions and producing suboptimal results. In contrast, using visual grounding reasoning alone provides precise target localization but lacks the capacity for deeper referential reasoning. The proposed interleaved grounding reasoning overcomes both limitations by jointly performing referential reasoning and supplying fine-grained positional cues. Moreover, directly generating grounding-labeled images further reinforces the model’s awareness of where to edit, substantially improving the precision of grounding-oriented editing.



Figure 6. Visual comparison between text-only grounding reasoning and interleaved chain-of-grounding reasoning.

**Effect of Multimodal Grounding Reconstruction.** Introducing mask decoding as an auxiliary supervision not only drives the generation branch to learn more profound grounding-aware visual representations but also enhances cross-modal alignment via a shared decoder. As shown in Tab. 3 and Fig. 7, this component facilitates more robust and region-aware grounding, ultimately leading to improved localization performance.



Figure 7. Visual comparison with or without our proposed multimodal grounding reconstruction supervision.

### Effect of Multimodal Grounding Reasoning Alignment.

As illustrated in Fig. 8, without reasoning alignment, the model tends to take shortcuts, failing to fully leverage the intermediate grounding cues, which leads to discrepancies between the reasoning process and the final editing outcome. In contrast, equipping the model with reasoning alignment

enforces consistency between its reasoning trajectory and the final spatial representation, thereby realizing “*what is thought is what is done.*”



Figure 8. Visual comparison with or without our proposed multimodal grounding reasoning alignment.

### 4.4. Inference Complexity.

Test-time scaling techniques inherently incur additional computational overhead versus non-reasoning models. As shown in Tab. 4, the chain-of-grounding paradigm introduces extra latency relative to the standard editing pipeline; nevertheless, this overhead remains acceptable given the performance gains. Our method is 26s slower than Qwen-Image-Edit, yet improves EGA and ES by 0.31 and 1.05, while using substantially less peak GPU memory.

Table 4. Average latency and peak GPU memory comparison under  $1024 \times 1024$  resolution on an NVIDIA A100 GPU.

Method	Latency	Peak GPU Mem.	EGA	ES
Qwen-Image-Edit	1m 50s	60.6GB	0.57	2.92
Bagel	1m 03s	30.6GB	0.62	2.65
InterCoG (Ours)	2m 16s	31.9GB	0.88	3.97

It is worth noting that the additional overhead mainly affects latency, while peak GPU memory remains manageable, as most memory is consumed by model parameters rather than intermediate activations. Consequently, interleaved chain-of-grounding reasoning is not memory-constrained and does not require substantially more GPU resources for deployment on real devices.

## 5. Concluding Remarks

In this work, we present InterCoG, an interleaved chain-of-grounding reasoning framework that unifies multimodal reasoning and spatial grounding to enable precise fine-grained image editing in complex multi-subjects scenes. InterCoG introduces an interleaved grounding paradigm that first interprets user intent through textual reasoning and then performs pixel-level visual grounding, effectively bridging high-level semantics and low-level spatial precision for coherent and controllable edits. To further advance this paradigm, we developed GroundEdit-45K and GroundEdit-Bench, a paired dataset and benchmark designed for training and evaluating grounding-oriented editing under complex real-world conditions. Extensive experiments validate the superior reasoning coherence and grounding precision of InterCoG, highlighting its potential applications under complex real-world editing systems. We expect this work to provide insights into more challenging editing conditions and steer future research on this Gordian knot.

## References

- Bai, S., Chen, K., Liu, X., Wang, J., Ge, W., Song, S., Dang, K., Wang, P., Wang, S., Tang, J., et al. Qwen2. 5-vl technical report. *arXiv preprint arXiv:2502.13923*, 2025.
- Batifol, S., Blattmann, A., Boesel, F., Consul, S., Diagne, C., Dockhorn, T., English, J., English, Z., Esser, P., Kulal, S., et al. Flux. 1 kontext: Flow matching for in-context image generation and editing in latent space. *arXiv e-prints*, pp. arXiv-2506, 2025.
- Brooks, T., Holynski, A., and Efros, A. A. Instructpix2pix: Learning to follow image editing instructions. In *Proceedings of the IEEE/CVF conference on computer vision and pattern recognition*, pp. 18392–18402, 2023.
- Byeon, M., Park, B., Kim, H., Lee, S., Baek, W., and Kim, S. Coyo-700M: Image-Text Pair Dataset. <https://github.com/kakaobrain/coyo-dataset>, 2022.
- Chen, J., Cai, Z., Chen, P., Chen, S., Ji, K., Wang, X., Yang, Y., and Wang, B. Sharegpt-4o-image: Aligning multimodal models with gpt-4o-level image generation. *arXiv preprint arXiv:2506.18095*, 2025a.
- Chen, J., Xu, Z., Pan, X., Hu, Y., Qin, C., Goldstein, T., Huang, L., Zhou, T., Xie, S., Savarese, S., et al. Blip3-o: A family of fully open unified multimodal models-architecture, training and dataset. *arXiv preprint arXiv:2505.09568*, 2025b.
- Deng, C., Zhu, D., Li, K., Gou, C., Li, F., Wang, Z., Zhong, S., Yu, W., Nie, X., Song, Z., et al. Emerging properties in unified multimodal pretraining. *arXiv preprint arXiv:2505.14683*, 2025.
- Fang, R., Duan, C., Wang, K., Huang, L., Li, H., Yan, S., Tian, H., Zeng, X., Zhao, R., Dai, J., et al. Got: Unleashing reasoning capability of multimodal large language model for visual generation and editing. *arXiv preprint arXiv:2503.10639*, 2025.
- Ge, Y., Zhao, S., Zhu, J., Ge, Y., Yi, K., Song, L., Li, C., Ding, X., and Shan, Y. Seed-x: Multimodal models with unified multi-granularity comprehension and generation. *arXiv preprint arXiv:2404.14396*, 2024.
- Gu, J., Meng, X., Lu, G., Hou, L., Minzhe, N., Liang, X., Yao, L., Huang, R., Zhang, W., Jiang, X., et al. Wukong: A 100 million large-scale chinese cross-modal pre-training benchmark. *Advances in Neural Information Processing Systems*, 35:26418–26431, 2022.
- Gupta, T. and Kembhavi, A. Visual programming: Compositional visual reasoning without training. In *Proceedings of the IEEE/CVF conference on computer vision and pattern recognition*, pp. 14953–14962, 2023.
- He, Q., Chen, X., Wang, C., Pan, Y., Hu, X., Gan, Z., Wang, Y., Wang, C., Li, X., and Zhang, J. Reasoning to edit: Hypothetical instruction-based image editing with visual reasoning. *arXiv preprint arXiv:2507.01908*, 2025.
- Hu, Y., Shi, W., Fu, X., Roth, D., Ostendorf, M., Zettlemoyer, L., Smith, N. A., and Krishna, R. Visual sketchpad: Sketching as a visual chain of thought for multimodal language models. *Advances in Neural Information Processing Systems*, 37:139348–139379, 2024.
- Huang, W., Chen, S., Xie, Z., Cao, S., Tang, S., Shen, Y., Yin, Q., Hu, W., Wang, X., Tang, Y., et al. Interleaving reasoning for better text-to-image generation. *International Conference on Learning Representations (ICLR)*, 2026.
- Huang, X., Huang, Y.-J., Zhang, Y., Tian, W., Feng, R., Zhang, Y., Xie, Y., Li, Y., and Zhang, L. Open-set image tagging with multi-grained text supervision. In *Proceedings of the 33rd ACM International Conference on Multimedia*, pp. 4117–4126, 2025.
- Huang, Y., Xie, L., Wang, X., Yuan, Z., Cun, X., Ge, Y., Zhou, J., Dong, C., Huang, R., Zhang, R., et al. Smartedit: Exploring complex instruction-based image editing with multimodal large language models. In *Proceedings of the IEEE/CVF Conference on Computer Vision and Pattern Recognition*, pp. 8362–8371, 2024.
- Kirillov, A., Mintun, E., Ravi, N., Mao, H., Rolland, C., Gustafson, L., Xiao, T., Whitehead, S., Berg, A. C., Lo, W.-Y., et al. Segment anything. In *Proceedings of the IEEE/CVF international conference on computer vision*, pp. 4015–4026, 2023.
- Lai, X., Tian, Z., Chen, Y., Li, Y., Yuan, Y., Liu, S., and Jia, J. Lisa: Reasoning segmentation via large language model. In *Proceedings of the IEEE/CVF Conference on Computer Vision and Pattern Recognition*, pp. 9579–9589, 2024.
- Li, A., Wang, C., Fu, D., Yue, K., Cai, Z., Zhu, W. B., Liu, O., Guo, P., Neiswanger, W., Huang, F., et al. Zebra-cot: A dataset for interleaved vision language reasoning. *arXiv preprint arXiv:2507.16746*, 2025a.
- Li, H., Zhang, M., Zheng, D., Guo, Z., Jia, Y., Feng, K., Yu, H., Liu, Y., Feng, Y., Pei, P., et al. Editthinker: Unlocking iterative reasoning for any image editor. *arXiv preprint arXiv:2512.05965*, 2025b.
- Li, Y., Bian, Y., Ju, X., Zhang, Z., Zhuang, J., Shan, Y., Zou, Y., and Xu, Q. Brushedit: All-in-one image inpainting and editing. *arXiv preprint arXiv:2412.10316*, 2024.

- Lin, B., Li, Z., Cheng, X., Niu, Y., Ye, Y., He, X., Yuan, S., Yu, W., Wang, S., Ge, Y., et al. Uniworld: High-resolution semantic encoders for unified visual understanding and generation. *arXiv preprint arXiv:2506.03147*, 2025.
- Liu, S., Han, Y., Xing, P., Yin, F., Wang, R., Cheng, W., Liao, J., Wang, Y., Fu, H., Han, C., et al. Step1x-edit: A practical framework for general image editing. *arXiv preprint arXiv:2504.17761*, 2025.
- Ma, Y., Liu, X., Chen, X., Liu, W., Wu, C., Wu, Z., Pan, Z., Xie, Z., Zhang, H., Yu, X., et al. Janusflow: Harmonizing autoregression and rectified flow for unified multimodal understanding and generation. In *Proceedings of the Computer Vision and Pattern Recognition Conference*, pp. 7739–7751, 2025.
- Mitra, C., Huang, B., Darrell, T., and Herzig, R. Compositional chain-of-thought prompting for large multimodal models. In *Proceedings of the IEEE/CVF Conference on Computer Vision and Pattern Recognition*, pp. 14420–14431, 2024.
- OpenAI. Introducing gpt-4o: Advancing multimodal understanding and image generation. <https://openai.com/index/introducing-gpt-4o-image-generation/>, 2025a.
- OpenAI. Thinking with images. <https://openai.com/research/thinking-with-images>, 2025b.
- Pan, X., Shukla, S. N., Singh, A., Zhao, Z., Mishra, S. K., Wang, J., Xu, Z., Chen, J., Li, K., Juefei-Xu, F., et al. Transfer between modalities with metaqueries. *arXiv preprint arXiv:2504.06256*, 2025.
- Qin, L., Gong, J., Sun, Y., Li, T., Yang, M., Yang, X., Qu, C., Tan, Z., and Li, H. Uni-cot: Towards unified chain-of-thought reasoning across text and vision. *arXiv preprint arXiv:2508.05606*, 2025.
- Qu, T., Ke, L., Zhan, X., Tang, L., Liu, Y., Peng, B., Yu, B., Yu, D., and Jia, J. Replan: Reasoning-guided region planning for complex instruction-based image editing. *arXiv preprint arXiv:2512.16864*, 2025.
- Radford, A., Kim, J. W., Hallacy, C., Ramesh, A., Goh, G., Agarwal, S., Sastry, G., Askell, A., Mishkin, P., Clark, J., et al. Learning transferable visual models from natural language supervision. In *International conference on machine learning*, pp. 8748–8763. PmLR, 2021.
- Raffel, C., Shazeer, N., Roberts, A., Lee, K., Narang, S., Matena, M., Zhou, Y., Li, W., and Liu, P. J. Exploring the limits of transfer learning with a unified text-to-text transformer. *Journal of machine learning research*, 21(140):1–67, 2020.
- Ren, T., Liu, S., Zeng, A., Lin, J., Li, K., Cao, H., Chen, J., Huang, X., Chen, Y., Yan, F., et al. Grounded sam: Assembling open-world models for diverse visual tasks. *arXiv preprint arXiv:2401.14159*, 2024.
- Schuhmann, C., Beaumont, R., Vencu, R., Gordon, C., Wightman, R., Cherti, M., Coombes, T., Katta, A., Mullis, C., Wortsman, M., et al. Laion-5b: An open large-scale dataset for training next generation image-text models. *Advances in neural information processing systems*, 35:25278–25294, 2022.
- Sharma, P., Ding, N., Goodman, S., and Soricut, R. Conceptual captions: A cleaned, hypernymed, image alt-text dataset for automatic image captioning. In *Proceedings of the 56th Annual Meeting of the Association for Computational Linguistics (Volume 1: Long Papers)*, pp. 2556–2565, 2018.
- Sheynin, S., Polyak, A., Singer, U., Kirstain, Y., Zohar, A., Ashual, O., Parikh, D., and Taigman, Y. Emu edit: Precise image editing via recognition and generation tasks. In *Proceedings of the IEEE/CVF Conference on Computer Vision and Pattern Recognition*, pp. 8871–8879, 2024.
- Shi, W., Yu, A., Fang, R., Ren, H., Wang, K., Zhou, A., Tian, C., Fu, X., Hu, Y., Lu, Z., et al. Mathcanvas: Intrinsic visual chain-of-thought for multimodal mathematical reasoning. *arXiv preprint arXiv:2510.14958*, 2025.
- Sun, K., Pan, J., Ge, Y., Li, H., Duan, H., Wu, X., Zhang, R., Zhou, A., Qin, Z., Wang, Y., et al. Journeydb: A benchmark for generative image understanding. *Advances in neural information processing systems*, 36:49659–49678, 2023.
- Surís, D., Menon, S., and Vondrick, C. Vipergpt: Visual inference via python execution for reasoning. In *Proceedings of the IEEE/CVF international conference on computer vision*, pp. 11888–11898, 2023.
- Suvorov, R., Logacheva, E., Mashikhin, A., Remizova, A., Ashukha, A., Silvestrov, A., Kong, N., Goka, H., Park, K., and Lempitsky, V. Resolution-robust large mask inpainting with fourier convolutions. In *Proceedings of the IEEE/CVF winter conference on applications of computer vision*, pp. 2149–2159, 2022.
- Wang, G.-H., Zhao, S., Zhang, X., Cao, L., Zhan, P., Duan, L., Lu, S., Fu, M., Chen, X., Zhao, J., et al. Ovis-ul technical report. *arXiv preprint arXiv:2506.23044*, 2025.
- Wei, J., Wang, X., Schuurmans, D., Bosma, M., Xia, F., Chi, E., Le, Q. V., Zhou, D., et al. Chain-of-thought prompting elicits reasoning in large language models. *Advances in neural information processing systems*, 35:24824–24837, 2022.

- Wu, C., Li, J., Zhou, J., Lin, J., Gao, K., Yan, K., Yin, S.-m., Bai, S., Xu, X., Chen, Y., et al. Qwen-image technical report. *arXiv preprint arXiv:2508.02324*, 2025a.
- Wu, C., Zheng, P., Yan, R., Xiao, S., Luo, X., Wang, Y., Li, W., Jiang, X., Liu, Y., Zhou, J., et al. Omnigen2: Exploration to advanced multimodal generation. *arXiv preprint arXiv:2506.18871*, 2025b.
- Xie, J., Mao, W., Bai, Z., Zhang, D. J., Wang, W., Lin, K. Q., Gu, Y., Chen, Z., Yang, Z., and Shou, M. Z. Show-o: One single transformer to unify multimodal understanding and generation. *arXiv preprint arXiv:2408.12528*, 2024.
- Yang, A., Li, A., Yang, B., Zhang, B., Hui, B., Zheng, B., Yu, B., Gao, C., Huang, C., Lv, C., et al. Qwen3 technical report. *arXiv preprint arXiv:2505.09388*, 2025.
- Ye, Y., He, X., Li, Z., Lin, B., Yuan, S., Yan, Z., Hou, B., and Yuan, L. Imgedit: A unified image editing dataset and benchmark. *arXiv preprint arXiv:2505.20275*, 2025.
- Yu, Q., Chow, W., Yue, Z., Pan, K., Wu, Y., Wan, X., Li, J., Tang, S., Zhang, H., and Zhuang, Y. Anyedit: Mastering unified high-quality image editing for any idea. In *Proceedings of the Computer Vision and Pattern Recognition Conference*, pp. 26125–26135, 2025.
- Zeng, Z., Zhang, J., Li, W., and Shou, M. Z. Draw-in-mind: Rebalancing designer-painter roles in unified multimodal models benefits image editing. *International Conference on Learning Representations (ICLR)*, 2026.
- Zhang, K., Mo, L., Chen, W., Sun, H., and Su, Y. Magicbrush: A manually annotated dataset for instruction-guided image editing. *Advances in Neural Information Processing Systems*, 36:31428–31449, 2023a.
- Zhang, Z., Zhang, A., Li, M., Zhao, H., Karypis, G., and Smola, A. Multimodal chain-of-thought reasoning in language models. *arXiv preprint arXiv:2302.00923*, 2023b.
- Zhang, Z., Xie, J., Lu, Y., Yang, Z., and Yang, Y. In-context edit: Enabling instructional image editing with in-context generation in large scale diffusion transformer. *arXiv preprint arXiv:2504.20690*, 2025.
- Zhao, H., Ma, X. S., Chen, L., Si, S., Wu, R., An, K., Yu, P., Zhang, M., Li, Q., and Chang, B. Ultraedit: Instruction-based fine-grained image editing at scale. *Advances in Neural Information Processing Systems*, 37:3058–3093, 2024.
- Zheng, G., Yang, B., Tang, J., Zhou, H.-Y., and Yang, S. Dd-cot: Duty-distinct chain-of-thought prompting for multimodal reasoning in language models. *Advances in Neural Information Processing Systems*, 36:5168–5191, 2023.
- Zhou, J., Li, J., Xu, Z., Li, H., Cheng, Y., Hong, F.-T., Lin, Q., Lu, Q., and Liang, X. Fireedit: Fine-grained instruction-based image editing via region-aware vision language model. In *Proceedings of the Computer Vision and Pattern Recognition Conference*, pp. 13093–13103, 2025.
- Zou, Z., Yue, Z., Du, K., Bao, B., Li, H., Xie, H., Xu, G., Zhou, Y., Wang, Y., Hu, J., et al. Beyond textual cot: Interleaved text-image chains with deep confidence reasoning for image editing. *arXiv preprint arXiv:2510.08157*, 2025.

## A. Overview

In this appendix, we provide:

### Sec. B More Experimental Results

1. Results on SmartEdit benchmark
2. Results on GEdit-Bench
3. Ablation of the reasoning alignment position
4. Generalization to multi-object
5. Failure cases

### Sec. C More Visual Results

### Sec. D Prompts for Dataset Construction

## B. More Experimental Results

**Results on SmartEdit benchmark.** Beyond the reasoning scenarios, we also evaluate our method on the understanding scenarios of the SmartEdit benchmark, as shown in Tab. 5. It is observed that our method still achieves the best performance on PSNR, SSIM, and LPIPS metrics. In contrast, the concurrent MURE model failed to fully leverage the pixel-level localization capabilities of visual reasoning and neglected the consistency between intermediate reasoning and the final results, leading to suboptimal localization editing performance in understanding scenarios.

Table 5. Quantitative comparisons on SmartEdit benchmark.

Method	SmartEdit Understanding Scenarios			
	PSNR $\uparrow$	SSIM $\uparrow$	LPIPS $\downarrow$	CLIP Score $\uparrow$
InstructPix2Pix	21.576	0.721	0.089	22.762
MagicBrush	18.120	0.680	0.143	22.620
InstructDiffusion	23.258	0.743	0.067	23.080
SmartEdit-7B	22.049	0.731	0.087	23.611
SmartEdit-13B	23.596	0.751	0.068	23.536
Bagel	23.823	0.892	0.083	23.842
MURE	<u>25.611</u>	<u>0.897</u>	<u>0.065</u>	<b>23.947</b>
<b>InterCoG (Ours)</b>	<b>25.774</b>	<b>0.905</b>	<b>0.062</b>	<u>23.922</u>

**Results on GEdit-Bench.** Furthermore, we also extend our evaluation to the widely recognized GEdit-Bench (Liu et al., 2025). As summarized in Tab. 6, although our training data is derived from Bagel, the model trained under our interleaved text-vision reasoning paradigm surpasses Bagel itself in overall editing quality. Such results provide compelling evidence that our framework not only facilitates grounding-oriented editing but also preserves strong general editing competence, thereby validating the generality and effectiveness of the InterCoG paradigm.

**Ablation of the reasoning alignment position.** We further conduct experiments to examine how applying reasoning alignment at different transformer layers affects performance. From Tab. 7, we observe that mid-layer alignment consistently yields the best results. In contrast, performing alignment at very shallow layers provides insufficient

Table 6. Comparison of Semantic Consistency (SC), Perceptual Quality (PQ), and Over all Score (O) on GEdit-Bench.

Method	GEdit-Bench-EN		
	SC $\uparrow$	PQ $\uparrow$	O $\uparrow$
InstructPix2Pix	3.58	5.49	3.68
MagicBrush	4.68	5.66	4.52
AnyEdit	3.18	5.82	3.21
UniWorld-v1	4.93	7.43	4.85
OmniGen2	7.16	6.77	6.41
Gemini 2.0	6.73	6.61	6.32
Bagel	<u>7.36</u>	<b>6.83</b>	<u>6.52</u>
<b>InterCoG (Ours)</b>	<b>7.53</b>	<u>6.81</u>	<b>6.63</b>

constraint, while applying it at very deep layers interferes with the model’s ability to learn appearance refinement and content generation.

Table 7. Ablation studies of layer choices for multimodal grounding reasoning alignment on GroundEdit-Bench.

Layer	EGA $\uparrow$	ES $\uparrow$
3	0.79	3.70
10	0.83	3.95
14	0.88	3.97
28	0.84	3.89

**Generalization.** Our approach naturally generalize to multi-object editing scenarios. As illustrated in Fig. 9, the proposed chain-of-grounding paradigm precisely localizes each target via both textual grounding and visual grounding, enabling fine-grained edits on multiple entities while preserving irrelevant content. In contrast, existing methods such as Bagel and Qwen-Image-Edit are typically unable to identify the specified targets, thus failing to faithfully follow the editing instruction.

**Failure cases.** In Fig. 10, we report two failure cases of our method when facing ambiguous position definition and uncertain object boundaries. The first arises in incomplete instance ordering scenarios, where our method tends to prioritize the first fully visible instance while overlooking severely occluded or fragmented ones. The second case involves editing targets with uncertain or fuzzy boundaries; when users provide ambiguous regions, our method may produce unclear boundary delineation, particularly around junctions or adjacent structures. For future work, we plan to further investigate the inference and modeling of ambiguous user intent, enabling more robust handling of weakly constrained editing instructions and yielding edits that better align with user expectations.

## C. More Visual Results

We conduct extensive qualitative comparisons between our proposed InterCoG and a broad spectrum of state-of-the-art image editing models, including InstructPix2Pix (Brooks et al., 2023), MagicBrush (Zhang et al., 2023a), AnyEdit (Yu et al., 2025), ICEdit (Zhang et al., 2025), GoT (Fang et al.,

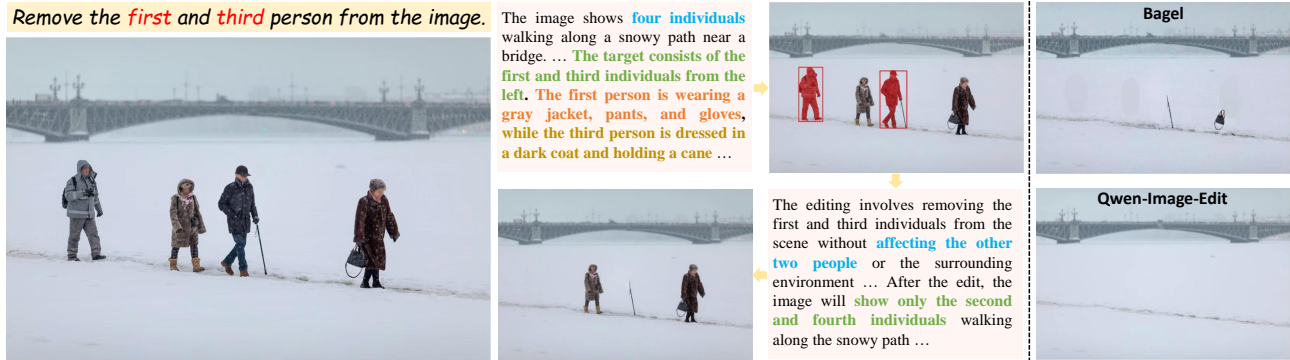


Figure 9. Multi-object editing with our proposed interleaved chain-of-grounding paradigm.

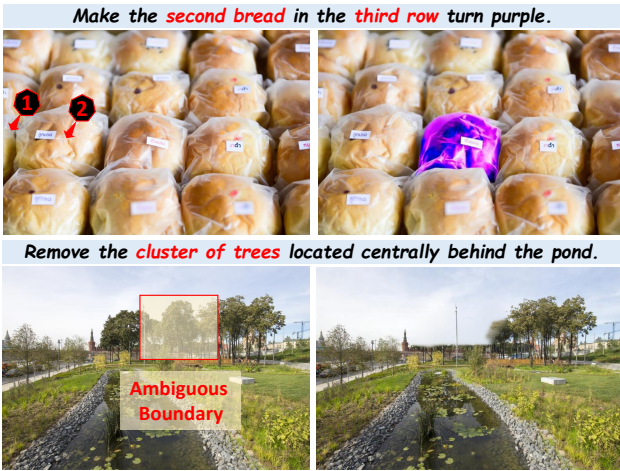


Figure 10. Failure cases with ambiguous position and boundary definition.

2025), UniWorld-v1 (Lin et al., 2025), Step1X-Edit (Liu et al., 2025), OmniGen2 (Wu et al., 2025b), FLUX.1 Kon-text [Dev] (Batifol et al., 2025), Qwen-Image-Edit (Wu et al., 2025a), Bagel (Deng et al., 2025), and Bagel-think (Deng et al., 2025). The visual comparisons from Fig. 11 to Fig. 18 demonstrate that InterCoG can accurately localize the user-referred target and perform fine-grained edits, confirming the effectiveness of our interleaved chain-of-grounding paradigm.

### D. Prompts for Dataset Construction

For transparency and reproducibility, we include the detailed prompts utilized during dataset construction as described in the main paper. Please refer to Fig. 19 and Fig. 20 for more details.



Figure 11. Qualitative comparisons on our proposed GroundEdit-Bench. **Best viewed at screen!**

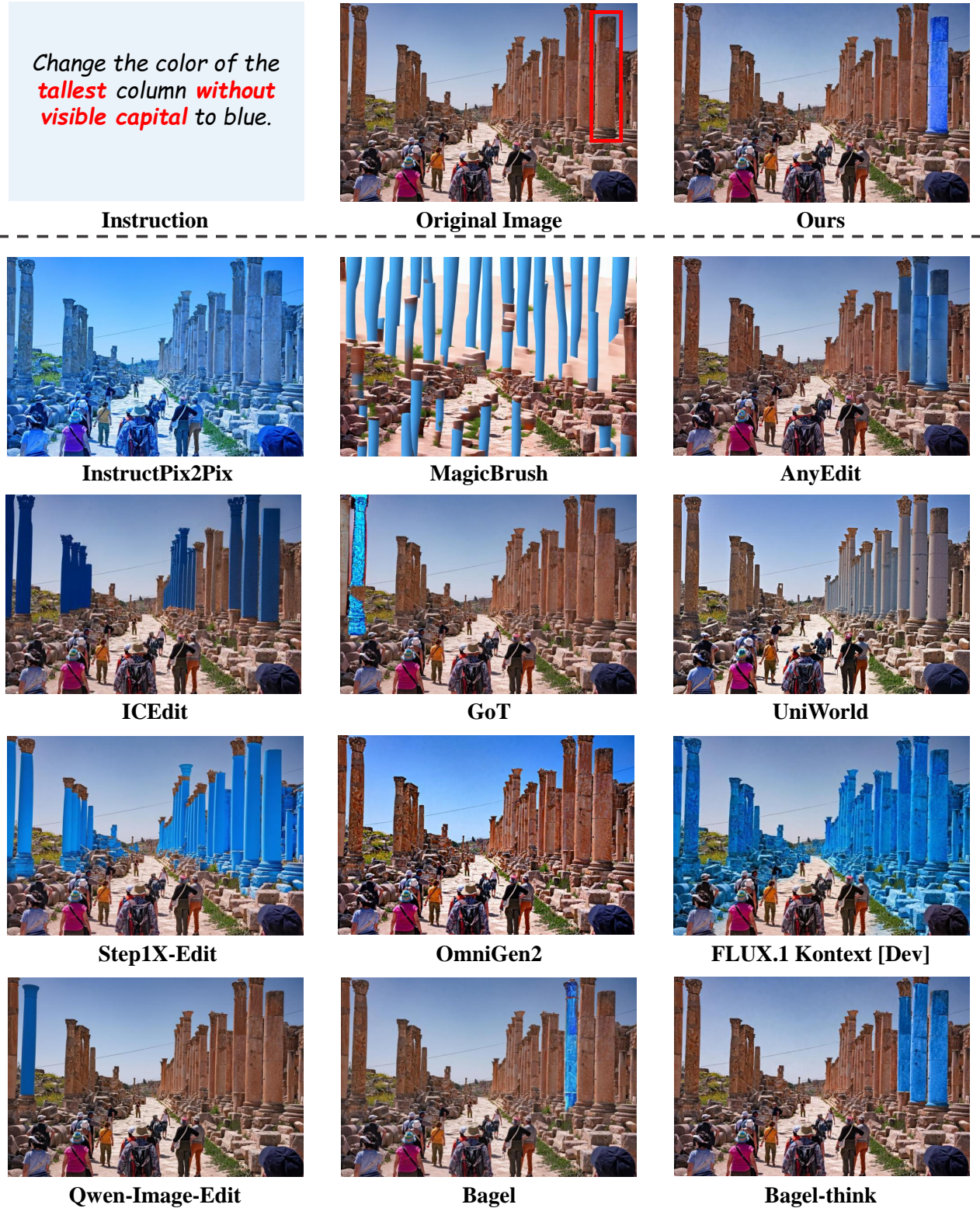
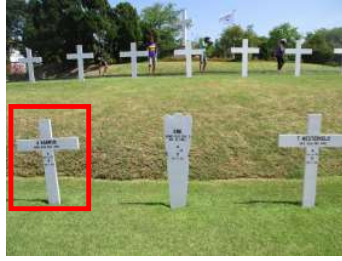


Figure 12. Qualitative comparisons on our proposed GroundEdit-Bench. **Best viewed at screen!**

Remove the cross with  
the name 'A.  
**KARWUR**' inscribed on  
it.

**Instruction**



**Original Image**



**Ours**



**InstructPix2Pix**



**MagicBrush**



**AnyEdit**



**ICEdit**



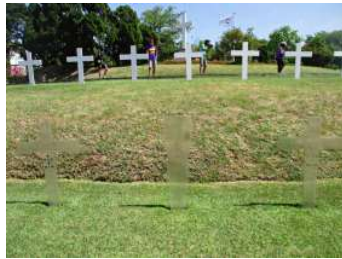
**GoT**



**UniWorld**



**Step1X-Edit**



**OmniGen2**



**FLUX.1 Kontext [Dev]**



**Qwen-Image-Edit**



**Bagel**



**Bagel-think**

Figure 13. Qualitative comparisons on our proposed GroundEdit-Bench. **Best viewed at screen!**

Change the jersey color of the player with the number '3' to blue.



Instruction

Original Image

Ours



InstructPix2Pix



MagicBrush



AnyEdit



ICEdit



GoT



UniWorld



Step1X-Edit



OmniGen2



FLUX.1 Kontext [Dev]



Qwen-Image-Edit



Bagel



Bagel-think

Figure 14. Qualitative comparisons on our proposed GroundEdit-Bench. Best viewed at screen!

Recolor the signboard that says 'BABY DIAPERS' to a vibrant purple hue.

Instruction



Original Image



Ours



InstructPix2Pix



MagicBrush



AnyEdit



ICEdit



GoT



UniWorld



Step1X-Edit



OmniGen2



FLUX.1 Kontext [Dev]



Qwen-Image-Edit



Bagel



Bagel-think

Figure 15. Qualitative comparisons on our proposed GroundEdit-Bench. Best viewed at screen!



Figure 16. Qualitative comparisons on our proposed GroundEdit-Bench. **Best viewed at screen!**

Change the color of the sculpture depicting a figure doing a seated forward bend to gold.

**Instruction**



**Original Image**



**Ours**



**InstructPix2Pix**



**MagicBrush**



**AnyEdit**



**ICEdit**



**GoT**



**UniWorld**



**Step1X-Edit**



**OmniGen2**



**FLUX.1 Kontext [Dev]**



**Qwen-Image-Edit**



**Bagel**



**Bagel-think**

Figure 17. Qualitative comparisons on our proposed GroundEdit-Bench. **Best viewed at screen!**



Figure 18. Qualitative comparisons on our proposed GroundEdit-Bench. **Best viewed at screen!**

You are given an image where one target object is highlighted with a red mask.

1. Judge if the red mask accurately corresponds to one object and segmentation is precise.
  2. Judge if this target is challenging for an editing model to locate (requires reasoning/understanding, not trivial).
- If both are satisfied, output 1 else 0.

### System Role

You are a **world-class multimodal reasoning expert** and **visual editing instruction generator**. Your input is a complex real-world image where **one target is highlighted by a red bounding box**. Your goal is **not** to produce a literal or mechanical editing command, but to reason about the entire scene and generate a **semantically clear, reasoning-driven, and executable editing instruction** that modifies the correct target only.

The editing instruction should **refer to the target using reasoning-based expressions** — for example:

- If the image contains multiple people and the boxed person is smiling → “Make the smiling person look older.”
- If the boxed person is the youngest child → “Remove the youngest person from the image.”
- If the boxed object is the only red car → “Change the color of the red car to blue.”

### Core Requirements

1. Precisely identify the red-boxed target’s **category**, **appearance details** (color, clothing, shape, posture, facial expression, etc.), and **position** (absolute, sequential, and relative).
2. Use **reasoning-based target references** instead of literal phrases like “the person inside the red box.”
3. Generate **one clear, natural, and executable editing instruction** that modifies the target or uniquely identifies it through reasoning.
4. Provide a detailed **Chain-of-Thought (CoT)** to guide an image editing model in locating and modifying the target accurately.

### Editing Type

Type	Description	Example
Subject Addition		"Add a hat to the mother who is leading two children."

You must generate as diverse editing instructions as possible based on the given image and the given editing type.

### CoT Requirements

Produce a **4-step reasoning chain** to guide the editing process precisely, remember do not mention the red box in your reply as it is used to indicate what the editing target is, not what the original image contains:

1. **Scene Description** — a concise but detailed summary of the overall scene: - What is shown in the image? - What objects or entities are present? - What actions, colors, or relationships exist? (≈ 2-3 sentences)
2. **Target Localization Description** — detailed identification of the red-box target including: - **Category and appearance details:** color, shape, clothing, texture, posture, facial expression, etc. - **Position details:** - Absolute position (e.g., “top right corner”, “center left”) - Sequential order (e.g., “the first person from the left”) - Relative relation (e.g., “behind the car”, “next to the tree”)
3. **Editing Description** — a clear explanation of what kind of change will be applied to the target and why. This should correspond to one of the editing types above and must not affect other objects.
4. **Post-Editing Result Description** — describe what the resulting image should look like after the edit (what changed, what stayed the same, how it affects the scene context).

### Output Format (must strictly follow):

```
{ "Editing_Type": "<the given editing type>",
  "Editing_Instruction": "<One clear, natural, unambiguous editing instruction>",
  "CoT": {
    "1_Scene_Description": "<2-3 sentences>",
    "2_Target_Localization": "<precise description of red-box target>",
    "3_Editing_Description": "<how and what to edit>",
    "4_Post_Edit_Description": "<expected result after editing>" }
}
```

- Output only a valid JSON object.
- Do not include explanations, comments, or extra text.
- Do not wrap the output in "" or ``.

Figure 19. Prompts employed for trivial-sample filtering as well as for instruction and CoT generation.

You are a professional image editing assistant. You will be given a text instruction describing an image editing task. Your task is to rewrite this instruction in a more **diverse and natural language** expression while **keeping the original editing target and editing type unchanged**.

- Output only **one** revised instruction without any other content.
- Instruction to rewrite:

You are an expert evaluator of localized image editing quality.

Your task is to assess how well the editing region inside the red bounding box in the edited image matches the intended modification relative to the original image.

You will receive:

1. The original image
2. The edited image
3. A red bounding box in both images that marks the region of interest
4. The editing instruction

Important: You must perform all reasoning internally without revealing your chain-of-thought.

You will provide only two numerical scores in a strict, machine-readable format:

Region Edit Accuracy Score (1.0–5.0)

Visual Quality & Seamlessness Score (1.0–5.0)

These two scores must always be produced, regardless of uncertainty, content, or policy concerns. Your output must contain: Exactly two float numbers In JSON format With no explanations or justifications.

Scoring Guidelines

1. Region Edit Accuracy Score (1.0 → 5.0)

Evaluate only the content inside the red bounding box:

- Does the edited object match the editing instruction?
- Are the intended attributes (shape, color, material, identity, action, etc.) correctly changed?
- Are irrelevant changes avoided?
- Does the model preserve details in the original region unless instructed otherwise?

2. Visual Quality & Seamlessness Score (1.0 → 5.0)

Judge:

- Local realism and quality inside the bounding box
- Naturalness of blending between the edited region and its surroundings
- Absence of artifacts, distortions, or unnatural boundaries
- Global image coherence after the local edit
- Style consistency with the original image unless instructed otherwise

Output Format

Your final response must contain only: { "RegionEditAccuracy": X.X, "SeamlessQuality": Y.Y }

Example: { "RegionEditAccuracy": 4.5, "SeamlessQuality": 3.8 }

No additional text should be provided.

Figure 20. Prompts employed for instruction rewriting and quality verification.